CrossMark

ORIGINAL ARTICLE

Prospective head-to-head comparison of ^{11}C-choline-PET/MR and ^{11}C-choline-PET/CT for restaging of biochemical recurrent prostate cancer

Matthias Eiber[1,2] · Isabel Rauscher[1] · Michael Souvatzoglou[1] · Tobias Maurer[3] ·
Markus Schwaiger[1] · Konstantin Holzapfel[4] · Ambros J. Beer[1,5]

Abstract

Purpose Whole-body integrated ^{11}C-choline PET/MR might provide advantages compared to ^{11}C-choline PET/CT for restaging of prostate cancer (PC) due to the high soft-tissue contrast and the use of multiparametric MRI, especially for detection of local recurrence and bone metastases.

Materials and methods Ninety-four patients with recurrent PC underwent a single-injection/dual-imaging protocol with contrast-enhanced PET/CT followed by fully diagnostic PET/MR. Imaging datasets were read separately by two reader teams (team 1 and 2) assessing the presence of local recurrence, lymph node and bone metastases in predefined regions using a five-point scale. Detection rates were calculated. The diagnostic performance of PET/CT vs. PET/MR was compared using ROC analysis. Inter-observer and inter-modality variability, radiation exposure, and mean imaging time were evaluated. Clinical follow-up, imaging, and/or histopathology served as standard of reference (SOR).

Results Seventy-five patients qualified for the final image analysis. A total of 188 regions were regarded as positive: local recurrence in 37 patients, 87 regions with lymph node metastases, and 64 regions with bone metastases. Mean detection rate between both readers teams for PET/MR was 84.7% compared to 77.3% for PET/CT ($p > 0.05$). Local recurrence was identified significantly more often in PET/MR compared to PET/CT by team 1. Lymph node and bone metastases were identified significantly more often in PET/CT compared to PET/MR by both teams. However, this difference was not present in the subgroup of patients with PSA values ≤2 ng/ml.

Inter-modality and inter-observer agreement ($K > 0.6$) was moderate to substantial for nearly all categories. Mean reduction of radiation exposure for PET/MR compared to PET/CT was 79.7% (range, 72.6–86.2%). Mean imaging time for PET/CT was substantially lower (18.4 ± 0.7 min) compared to PET/MR (50.4 ± 7.9 min).

Conclusions ^{11}C-choline PET/MR is a robust imaging modality for restaging biochemical recurrent PC and interpretations between different readers are consistent. It provides a higher diagnostic value for detecting local recurrence compared to PET/CT with the advantage of substantial dose reduction. Drawbacks of PET/MR are a substantially longer imaging time and a slight inferiority in detecting bone and lymph node metastases in patients with PSA values >2 ng/ml. Thus, we suggest the use of ^{11}C-choline PET/MR especially for patients with low (≤2 ng/ml) PSA values, whereas PET/CT is preferable in the subgroup with higher PSA values.

Konstantin Holzapfel and Ambros J. Beer share joint senior authorship.

Electronic supplementary material The online version of this article (doi:10.1007/s00259-017-3797-y) contains supplementary material, which is available to authorized users.

Matthias Eiber and Isabel Rauscher contributed equally to this work.

✉ Isabel Rauscher
  isabel.rauscher@tum.de

[1] Department of Nuclear Medicine, Technische Universität München, Klinikum rechts der Isar, Ismaninger Str. 22, 81675 Munich, Germany

[2] Department of Molecular and Medical Pharmacology, David Geffen School of Medicine at UCLA, Los Angeles, USA

[3] Department of Urology, Technische Universität München, Klinikum rechts der Isar, Ismaninger Str. 22, 81675 Munich, Germany

[4] Department of Radiology, Technische Universität München, Klinikum rechts der Isar, Ismaninger Str. 22, 81675 Munich, Germany

[5] Present address: Department of Nuclear Medicine, Ulm University, Albert-Einstein-Allee 23, 89081 Ulm, Germany

Introduction

Prostate cancer (PC) is the most frequent malignant tumor in elderly males and constitutes the third most common cause of cancer deaths in men in Europe [1, 2]. After primary treatment, relapse occurs within 10 years in 20–30% of patients who have undergone prostatectomy and within 5 years in up to 53% after external-beam radiotherapy [3–5]. Except for high PSA values, the diagnostic sensitivity of conventional imaging in the setting of PSA recurrence is often disappointing. However, positron emission tomography (PET) using different choline derivatives, especially ^{11}C-choline, has shown promising results in this context [6–8]. Moreover, hybrid positron emission tomography/computed tomography (PET/CT) has further improved diagnostic performance in recurrent PC, as it facilitates anatomical localization of PET-positive findings and provides additional morphological information (e.g., lymph node size, osteoblastic bone metastases) [9]. However, in cases with low PSA values (especially <1–2 ng/ml), there is still a substantial number of patients for which no correlate for the PSA increase can be found [6, 10–13].

The recent introduction of PET/MR (positron emission tomography/magnetic resonance imaging) scanners offers the possibility to combine the molecular information of PET both with the high soft-tissue contrast and the functional information of MR [14, 15]. Functional MR tools like DCE (dynamic contrast enhanced)-MRI or DWI-(diffusion weighted)-MRI have been shown to add information for restaging of PC patients, especially due to the high sensitivity of DCE MRI for detection of local recurrence [16–19]. For bone metastases in general, a prior study using ^{18}F-FDG has shown a higher diagnostic accuracy of PET/MR vs. PET/CT [20]. Moreover, known limitations of PET/MR in oncologic patients like detection of small lung metastases are of less relevance in this patient group as pulmonary metastases from PC are rare and when present usually large enough to be picked up by PET/MR [21]. Thus, an increase in the diagnostic performance by PET/MR compared to PET/CT can be hypothesized in this patient population. However, PET/MR is also a challenging technology with several known disadvantages compared to PET/CT, like complex scan protocols with long imaging times, issues with patient comfort and high demands for the imaging specialists concerning interpretation of the vast amount of multiparametric multimodal data [22].

Thus, the aim of this study was a comprehensive prospective evaluation of the performance of ^{11}C-choline PET/MR compared to ^{11}C-choline PET/CT in restaging of recurrent PC in a well-defined patient population. Outcome measurements were (a) overall detection rates, regional lesion detection efficacy and inter-observer and inter-modality agreement to compare diagnostic performance and reliability and (b) analyses of imaging time and radiation exposure to quantify relevant methodological differences for this specific clinical indication.

Materials and methods

All patients between July 2011 and May 2013 routinely scheduled for restaging of PC were eligible for this prospective study. All patients gave informed consent. The study was approved by the institutional review board (IRB). Inclusion criteria for imaging were the lack of standard contraindications for MRI examinations, the ability to undergo a second examination after the PET/CT scan and the accessibility of the PET/MR scanner after the PET/CT scan. Patients underwent a dual-imaging/single-injection protocol consisting of a ^{11}C-choline PET/CT and followed by a ^{11}C-choline PET/MR with the smallest possible temporal delay in between. A total number of 94 patients underwent the dual-imaging/single-injection protocol. Only patients fulfilling all criteria for biochemical recurrence defined by the guidelines [13] were included and only one pair of scans was allowed per patient.

[11]C-choline PET/CT and PET/MR acquisition and image reconstruction

[11]C-choline was produced as described previously [6]. Patients fasted at least 6 h before ^{11}C-choline PET-scanning. Five minutes after injection of mean 777 ± 75 MBq ^{11}C-choline, patients underwent ^{11}C-choline PET/CT (pelvis to neck) on a Siemens Sensation 64 Biograph PET/CT scanner. First, a diagnostic CT scan was performed in the portal venous phase 80 s after intravenous injection of contrast agent (Imeron 300) (CareDose, 240 reference mAs, 120 kV, 0.5 s per rotation, 64×0.6 mm collimation) followed by the PET scan. A separate low-dose CT of the chest in deep inspiration was performed in all patients (25 mAs, 120 kV, 0.5 s per rotation, 64×0.6 mm collimation). All patients received diluted oral contrast (300 mg Telebrix) and a rectal filling with a negative contrast agent (100–150 ml ultrasound gel). All PET scans were acquired in 3D mode with an acquisition time of 3 min per bed position.

PET/MR was performed on a fully integrated whole-body hybrid PET/MR system (Siemens Biograph mMR, Siemens Healthcare, Erlangen, Germany). A detailed summary of the scanner's technical specifications and performance details has been published earlier [23]. PET/MR was acquired at a mean time of 49.1 ± 18.1 min after tracer injection (range, 23–118 min).

The PET/MR acquisition protocol was as follows: first, localizer MR sequences were acquired to determine the localization and number of PET bed positions. Then the PET

emission scans were initiated; emission time was 4 min per bed position covering the region from the pelvis to the neck in 3–4 bed positions. After an initial two-point T1-weighted coronal 3D VIBE sequence was acquired for attenuation correction, both a coronal T1w TSE and an axial T2w haste fat-saturated sequence were acquired simultaneously at every PET position. Then the pelvis was imaged with an axial T2w TSE, an axial DWI- (b = 50, 400 and 800 s/mm^2) and a DCE sequence during an additional PET acquisition over 15 min. Finally, the whole trunk was covered with contrast-enhanced, fat-saturated T1w VIBE sequences.

Notably, the different acquisition times for each bed position (3 min for PET/CT and 4 min for PET/MR) were not chosen to compensate for the later imaging point in PET/MR but rather related to the longer acquisition of MR sequences compared to contrast-enhanced CT and the pertinent consequence to use of this extra time to acquire simultaneous PET data.

Similar reconstruction methods were used for PET data acquired on the PET/CT and PET/MR scanners to maintain comparability. For both modalities, emission data was corrected for dead time, scatter, and random counts. Images were reconstructed iteratively by OSEM3D (ordered-subset expectation maximization) using three iterations and 21 subsets. Gaussian smoothing was applied (4 mm FWHM). The zoom factor was 1. For PET/MR data, attenuation maps were generated based on the water-weighted and fat-weighted MR Dixon images as described previously [24]. The required postprocessing software algorithm for attenuation correction of the PET/MR data operates automatically.

Image analysis

^{11}C-choline PET/CT and PET/MR were analyzed independently by two reader groups (reader team 1 and 2) consisting both of one board-certified nuclear medicine physician and one board-certified radiologist. In each group, the readers made their diagnoses in consensus and were blinded to the history of the patient except the former presence of PC with biochemical recurrence. PET/CT and PET/MR datasets were analyzed in random order with a time interval of at least 8 weeks in between. For each patient and imaging modality the presence of local recurrence, lymph node metastases, bone metastases, or other metastases were evaluated on a five-point scale: 1, definitely present; 2, probably present; 3, equivocal; 4, probably absent; and 5, definitely absent. As a comparison between single lymph node and bone metastases is not feasible, all lesions were assigned to a predefined set of regions (bone metastases: cervical, thoracic, lumbar spine, ribs, pelvis right and left side, upper or lower extremity; lymph node metastases: external, internal and common iliac vessel both right and left side, retroperitoneal, supradiaphragmatic).

Calculation of radiation dose and imaging time

Based on studies for biodistribution and radiation dosimetry of ^{11}C-choline, the effective dose in a human adult with a standard weight of 70 kg is 0.0044 mSv/MBq (internal exposure) [25]. Thus, the effective dose induced by injection of ^{11}C-choline (E_T) was calculated as: $E_T = \text{dose} \times 0.0044$ mSv/MBq. For calculation of effective external radiation exposure (E_{CT}) from the CT component of the PET/CT, the applied dose-length product (DLP) values were used to estimate the dose for each patient following the European Commission Guidelines on quality criteria for computed tomography: $E_{CT} = k \times \text{DLP}$ [26, 27]. DLP is a dose descriptor that depends on irradiated length, acquisition parameters (e.g., average effective mAs), and CT design. k is a conversion coefficient that is solely dependent on the anatomical region scanned. k values for standard anatomical regions in diagnostic CT have been published using the ICRP 60 tissue-weighting factors [27, 28]. A recent publication gives values for the new IRCP 103 tissue-weighting factor and recommended conversion factors for chest/abdomen/pelvis of 0.015 mSv × mGy-1 × cm-1 and for thorax of 0.014 mSv × mGy-1 × cm-1 [29].

For every patient, the imaging time needed for ^{11}C-choline PET/CT and ^{11}C-choline PET/MR was analyzed. It was calculated by the difference between the first sequence (scout scan in PET/CT, localizer in PET/MR) and the end of the acquisition (in PET/CT end of PET acquisition, in PET/MR end of last MR sequence).

Statistical analysis

Dichotomized data (1, definitely present and 2, probably present vs. 3, equivocal, 4, probably absent, and 5, definitely absent) were used to determined detection rates (number of patients with at least one positive finding) and detection efficacy for local recurrence, regional lymph node or bone metastases compared to the SOR. Comparison of proportions was performed using a Chi-squared test. To determine the discriminatory power for each method, receiver operating characteristic curve (ROC) analyses were performed both for the total number of regions evaluated as well as per region (local recurrence, lymph nodes, bones).

A kappa statistic was used to determine the inter-observer and inter-modality agreement for ^{11}C-choline PET/CT and PET/MR on a per-patient basis and a per-region basis. It was interpreted based on a classification provided by Landis and Koch: 0.0, poor; 0.0–0.20, slight; 0.21–0.40, fair; 0.41–0.60, moderate; 0.61–0.80, substantial; 0.81–1.00, almost-perfect reproducibility [30]. Descriptive analysis of imaging time and radiation dose for ^{11}C-choline PET/CT and PET/MR were performed. A p value less than 0.05 was considered statistically significant.
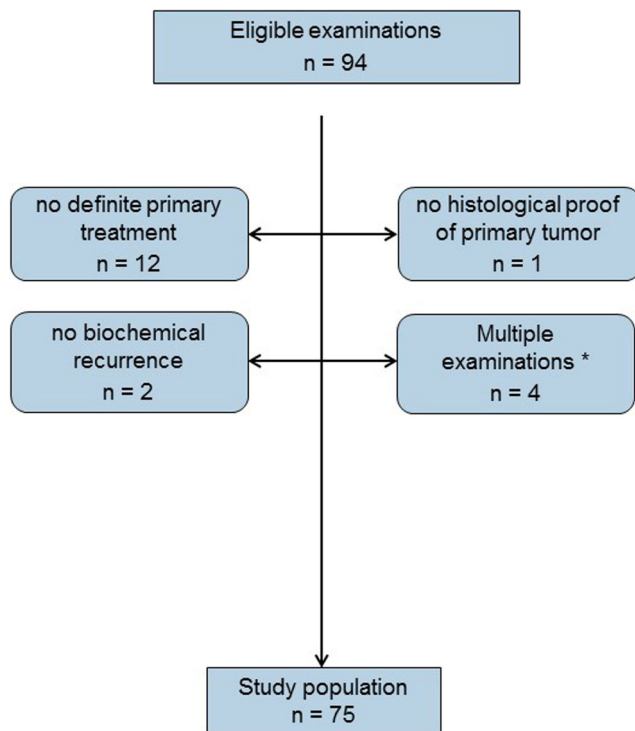
Fig. 1 Flow of patients in the study. * in cases where single patients underwent the single-injection dual-imaging protocol more than one time, only one examination of the patient was included in the analysis

Results

Patient characteristics and standard of reference (SOR)

Seventy-five of 94 patients fulfilled the criteria for final data analysis (Fig. 1). Median PSA value was 2.6 (range, 0.2–88) ng/ml. Detailed patient characteristics are presented in Table 1. Histopathological verification was performed in 19 of 75 patients. In patients without histopathology, standard of

Table 1 Patient characteristics

Number of patients	75
Primary radical prostatectomy (%)	76.0
Primary radiation therapy (%)	18.0
Primary hormone therapy (%)	5.3
Age in years	
Median (range)	70 (51–85)
Gleason score	
Median (range)	7 (5–9)
PSA (ng/ml)	
Median (range)	2.6 (0.2–88)
Interval: primary therapy – ^{11}C-choline PET-imaging (months)	
Median (range)	54 (2–276)

*In 25 of 75 patients, no information concerning the initial Gleason score could be obtained since the primary treatment of several patients dated back between 10 and 20 years

reference was defined by a tumor board consisting of a nuclear medicine physician, a radiologist, and a urologist performing a consensus reading using information from prior/subsequent imaging studies and/or clinical data (e.g., start of antihormonal therapy, radiation therapy). Mean follow-up time was 311 days (range, 63–535 days). Results were considered as malignant referring to the following criteria, which have been used in many recent studies on the diagnostic value of ^{11}C-choline PET: significant increase in PSA during follow-up or PSA doubling time < 10 months, confirmation or development of a detectable lesion in a site on a follow-up conventional imaging study or increase in lesion size on follow-up, decrease in PSA after irradiation, anti-androgen or another therapy [6, 31].

A total of 188 regions in 75 patients were finally judged as positive. Evidence of local recurrence was present in 37 out of 75 patients. Eighty-seven lymph nodes regions in 37 patients and 64 bone regions in 14 patients were regarded as positive. No visceral metastases (e.g., lungs, liver) were present.

Overall detection rate

Detection rate for ^{11}C-choline PET/CT was 77.3% (58/75 patients) for both reader teams. For ^{11}C-choline PET/MR mean detection rate was 84.7% with positive results in 84.0% (63/75 patients) for reader team 1 and 85.3% (64/75 patients) for reader team 2. Detection rates between ^{11}C-choline PET/CT and ^{11}C-choline PET/MR were not statistically different for either of the reader teams ($p = 0.4528$ and 0.5325, respectively). Positive findings only in PET/MR were detected by reader team 1 and 2 in nine patients (mean PSA value 1.8 and 2.5 ng/ml for reader team 1 and 2, respectively). Conversely positive findings only in PET/CT were present in four and three patients by reader team 1 and 2, respectively (mean PSA value 3.5 and 2.4 ng/ml for reader team 1 and 2, respectively).

Regional lesion detection

Diagnostic efficacy for ^{11}C-choline PET/CT and PET/MR detecting local recurrence, lymph node, and bone metastases based on regional analysis validated by SOR is given in Table 2. For the whole patient cohort, ^{11}C-choline PET/MR was more efficient in detection of local recurrence for both reader teams, but only statistical significantly different for one reader team. In contrast, lymph node and bone metastases were significantly more efficiently detected by ^{11}C-choline PET/CT compared to ^{11}C-choline PET/MR for both reader teams.

The detection of bone and lymph node metastases was more accurate using ^{11}C-choline PET/CT compared to PET/MR in the subgroup of patients with PSA values >2 ng/ml. The differences were statistically significant with the exception of bone metastases in reader group 1. No differences were observed for patients with a PSA value ≤2 ng/ml.

Table 2 Detection efficacy for local recurrence (LR), lymph node (LNM) and bone metastases (BM) by ^{11}C-choline PET/CT vs. PET/MR in all patients and stratified by PSA values. Dichotomized data with rating 1 and 2 scored as positive. Note that here the number of positive results validated by SOR are compared between both modalities in each reader team

	PET/CT (Reader team 1)	PET/MR (Reader team 1)	PET/CT (Reader team 2)	PET/MR (Reader team 2)
All patients				
LR ($n = 37$)	64.9% ($n = 24$)	97.3% ($n = 36$)	70.3% ($n = 26$)	86.5% ($n = 32$)
	$P = 0.001$[#]		$P = 0.167$	
LNM ($n = 87$)	85.1% ($n = 74$)	70.0% ($n = 60$)	81.6% ($n = 72$)	69.0% ($n = 60$
	$P = 0.014$*		$P = 0.047$*	
BM ($n = 64$)	89.1% ($n = 57$)	81.3% ($n = 52$)	96.9% ($n = 62$)	79.7% ($n = 51$)
	$P < 0.001$*		$P < 0.001$*	
PSA > 2 ng/ml				
LR ($n = 19$)	68.4% ($n = 13$)	100% ($n = 19$)	68.4% ($n = 13$)	84.2% ($n = 16$)
	$P = 0.026$[#]		$P = 0.445$	
LNM ($n = 69$)	88.4% ($n = 61$)	69.6% ($n = 48$)	85.5% ($n = 59$)	68.1% ($n = 47$)
	$P = 0.0123$*		$P = 0.0264$*	
BM ($n = 47$)	91.4% ($n = 43$)	80.6% ($n = 38$)	100% ($n = 47$)	80.8% ($n = 38$)
	$P = 0.2257$		$P = 0.0047$*	
PSA ≤ 2 ng/ml				
LR ($n = 18$)	61.1% ($n = 11$)	94.4% ($n = 17$)	72.2% ($n = 13$)	88.9% ($n = 16$)
	$P = 0.045$[#]		$P = 0.3983$	
LNM ($n = 18$)	72.2% ($n = 13$)	66.7% ($n = 12$)	72.2% ($n = 13$)	72.2% ($n = 13$)
	$P = 0.997$		$P = 0.710$	
BM ($n = 17$)	82.4% ($n = 14$)	82.4% ($n = 14$)	88.2% ($n = 15$)	76.5% ($n = 13$)
	$P = 0.653$		$P = 0.999$	

*Indicates statistically significant difference in favor of PET/CT

[#] Indicates statistically significant difference in favor of PET/MR

In both PSA subgroups, the detection of local recurrence was more efficient using ^{11}C-choline PET/MR compared to PET/CT. The differences were statistically significant for reader team 1 with a clear trend but not statistically significance for reader team 2. An example of a patient with local recurrence being detected both by ^{11}C-Choline PET/CT and PET/MR is illustrated in Fig. 2. An example of a patient with a lymph node metastasis and another one with a bone metastasis with discrepant ^{11}C-Choline PET/CT versus ^{11}C-Choline PET/MR images can be found in Fig. 3 and Figure 1S.

Data on the discriminatory power regarding reader confidence for local recurrence, lymph node, and bone metastases using ROC analysis for ^{11}C-choline PET/MR to PET/CT are presented in Table 3 and Table 1S. For lymph node and bone metastases, ^{11}C-choline PET/CT showed a statistically significant higher discriminatory value compared to ^{11}C-choline PET/MR in the entire patient cohort both for reader team 1 and 2 with the exception of bone metastases for reader team 2. The same result was observed in the subgroup of patients with a PSA value >2 ng/ml. No statistically significant differences were present in the subgroup of patients with PSA ≤2 ng/ml except for lymph node metastases for reader team 1.

Notably, the clearly higher diagnostic accuracy of ^{11}C-choline PET/MR vs. PET/CT for detection of local recurrence did not translate into a significant discriminatory value comparing the AUCs.

Inter-observer and inter-modality agreement

Cohen kappa statistics values showed a substantial inter-observer agreement between reader team 1 vs. 2 for ^{11}C-choline PET/CT and ^{11}C-choline PET/MR, respectively (Table 4). Data are presented both on patient base as well as separated for the different regions (local recurrence, lymph node, and bone metastases). Inter-modality agreement between results from ^{11}C-choline PET/CT and ^{11}C-choline PET/MR was substantial for both reader team with the exception of the evaluation of presence/absence of local recurrence.

PET/CT vs. PET/MR: Effective radiation dose and imaging time

Mean internal effective radiation dose for PET was 4.43 mSv (range, 2.47–4.06 mSv). Mean external effective dose by
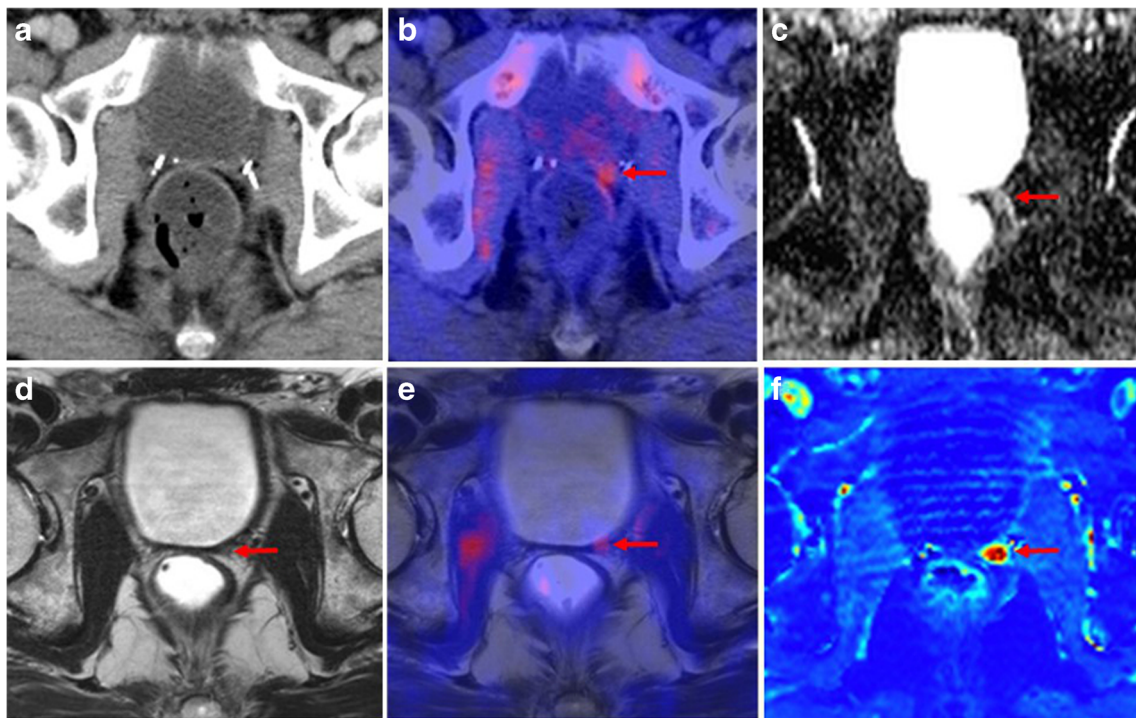
Fig. 2 Single-injection dual-imaging ^{11}C-choline PET/CT and PET/MR study in a 79-year-old patient with biochemical recurrent prostate cancer (PSA 1.7 ng/ml) after radical prostatectomy. Fused PET/CT (**b**, *red arrow*) and PET/MR (**e**, *red arrow*) show a faint left-sided choline uptake adjacent to the bladder, which raised the suspicion for local recurrence, but cannot be regarded as a definite diagnosis. As CT (**a**) did not provide a clear anatomical correlate, the lesion was judged in PET/CT as equivocal (score 3) by both reader teams. Final judgment in PET/MR was positive for both reader teams as additional information from multi-parametric MRI (increased wash-in rate in iAUC60 parametric map from dynamic contrast-enhanced imaging (**f**, *red arrow*), diffusion restriction in ADC map (**c**, *red arrow*)) clearly provided additional evidence for local recurrence apart from just morphological T2 TSE sequence (**D**, *red arrow*)(score 1)
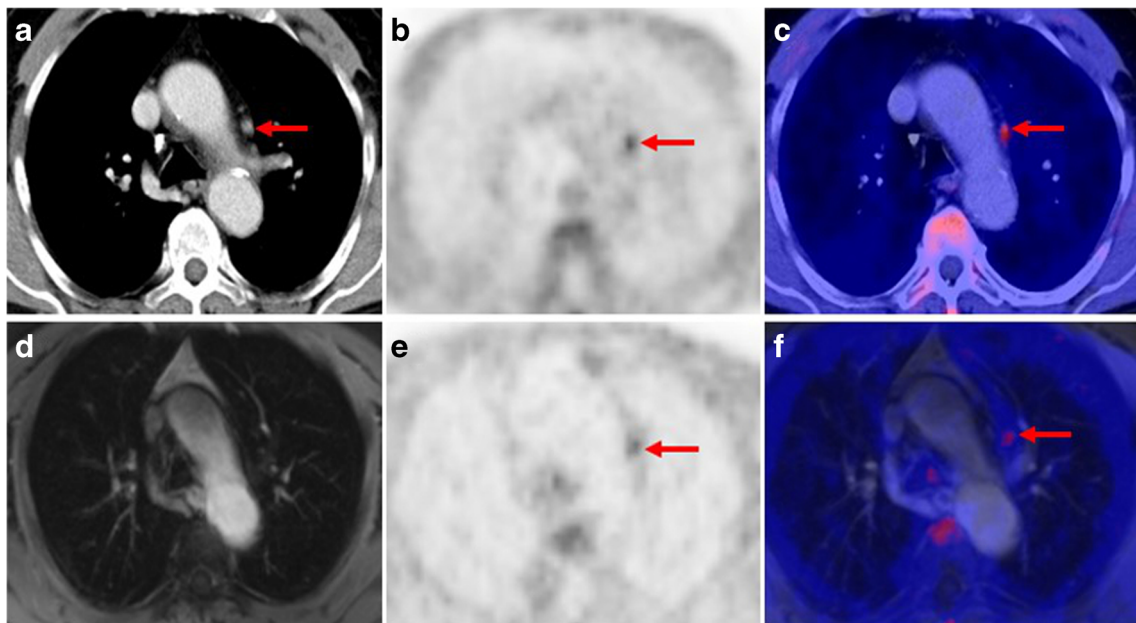

Fig. 3 ^{11}C-choline PET/CT and PET/MR in a 70-year-old patient with biochemical recurrent prostate cancer (PSA 1.5 ng/ml) after radical prostatectomy. Both PET of PET/CT (**b**, *red arrow*) and PET/MR (**e**, *red arrow*) showed a faint choline uptake in the aortopulmonary window. However, only in CT and fused PET/CT images the choline uptake was considered to be exactly in the location of a lymph node and was therefore judged as suspicious for lymph node metastasis (score 1, definitely present by both reader teams). Morphological contrast-enhanced T1 VIBE sequence (**d**) showed no clear morphological correlate. Therefore the faint uptake was misinterpreted as unspecific (score 5, definitely absent by both reader teams). Notably, in whole-body MRI anatomical delineation of small lymph nodes is often challenging compared to a regional dedicated MRI, which encompasses multiple sequences to optimally display all investigated structures

Table 3 Area under the curve for ^{11}C-choline PET/CT vs. PET/MR directly comparing the diagnostic performance by ROC analysis; 95% confidence intervals are given in *brackets*. Note that the ratings for every all pre-defined regions are compared for both modalities against the SOR in each reader team

	PET/CT Reader team 1	PET/CT Reader team 2	PET/MR Reader team 1	PET/MR Reader team 2
All patients				
local ($n = 75$)	0.914	0.872	0.956	0.918
	(0.827–0.967)	(0.774–0.938)	(0.881–0.990)	(0.831–0.969)
LN ($n = 600$)	0.959	0.937	0.842	0.863
	(0.939–0.937)*	(0.914–0.955)*	(0.810–0.870)	(0.833–0.889)
bone ($n = 730$)	0.956	0.984	0.908	0.919
	(0.938–0.970)	(0.972–0.992)*	(0.884–0.928)	(0.897–0.938)
PSA > 2 ng/ml				
LR ($n = 38$)	0.931	0.878	0.986	0.943
	(0.799–0.988)	(0.731–0.961)	(0.882–1)	(0.817–0.992)
LN ($n = 304$)	0.952	0.935	0.843	0.857
	(0.921–0.973)*	(0.901–0.960)*	(0.797–0.882)	(0.813–0.895)
bone ($n = 374$)	0.964	1	0.907	0.922
	(0.940–0.980)*	(0.990–1)*	(0.873–0.934)	(0.890–0.947)
PSA ≤ 2 ng/ml				
LR ($n = 37$)	0.893	0.864	0.923	0.885
	(0.748–0.970)	(0.711–0.954)	(0.786–0.985)	(0.737–0.966)
LN ($n = 296$)	0.982	0.939	0.939	0.884
	(0.960–0.994)*	(0.906–0.964)	(0.779–0.868)	(0.842–0.918)
bone ($n = 356$)	0.934	0.939	0.907	0.910
	(0.903–0.957)	(0.909–0.961)	(0.872–0.935)	(0.875–0.937)

*Indicates statistically significant difference in favor of PET/CT

diagnostic CT was 13.84 mSv (range, 8.62–23.26 mSv). This translates into a theoretical mean radiation exposure reduction for PET/MR compared to PET/CT of 79.7% (range, 72.6–86.2%). Mean imaging time for ^{11}C-choline PET/CT was statistical significantly lower compared to ^{11}C-choline PET/MR (18.4 min ± 0.7 min, range 17–21 min vs. 50.4 min ± 7.9 min, range 42–92 min, $p < 0.0001$, respectively).

Discussion

In this prospective study, we demonstrate in a relatively large, well-defined patient collective that ^{11}C-choline PET/MR is a robust imaging modality for restaging of biochemical recurrent PC with comparable results to PET/CT at a lower radiation exposure. PET/MR showed a higher overall detection rate on a per-patient basis, mainly due to the superiority in detection of local recurrence while PET/CT performed superior in the evaluation of lymph node and bone metastases in the patient group with PSA >2 ng/ml.

Detection of early recurrent prostate cancer is challenging for imaging. Recent advances are mainly based on the use of molecular imaging as well as mpMR. Notably, so far, no direct comparison of the diagnostic capability between hybrid ^{11}C-choline PET/CT with ^{11}C-choline PET/MR in a well-defined population of biochemical recurrent PC has been published. There are single reports on the technical aspects of using PET/MR, anatomical allocation of lesions or the comparison,

Table 4 Inter- and inter-modality agreement for ^{11}C-choline PET/CT and PET/MR

	PET/CT Reader team 1 vs. 2	PET/MR Reader team 1 vs. 2	PET/CT vs. PET/MR For reader team 1	PET/CT vs. PET/MR For reader team 2
All	0.751 ± 0.022	0.842 ± 0.024	0.645 ± 0.022	0.769 ± 0.024
LR	0.722 ± 0.093	0.691 ± 0.092	0.485 ± 0.082	0.575 ± 0.091
LN	0.735 ± 0.035	0.815 ± 0.038	0.649 ± 0.035	0.775 ± 0.037
Bone	0.737 ± 0.032	0.875 ± 0.034	0.636 ± 0.032	0.790 ± 0.034

± Indicates standard deviation

characterization of primary PC, and the correlation of different quantitative parameters in MR and PET with relatively inhomogeneous patient collectives in up to 32 patients [32–35].

As expected, but so far not prospectively evaluated, the highest difference in diagnostic performance was detectable for local recurrence. PET/MR proved to be superior to PET/CT, which is clearly attributed to the addition of functional MR imaging, especially DCE MRI. Kitajima et al. compared ^{11}C-choline PET/CT with pelvic mpMR for the detection of local recurrence and concluded that mpMR is superior to ^{11}C-choline PET/CT just as our study results suggest [36]. Further, several MR-only studies proved that DCE-MRI is a valid and efficient tool for detecting PC recurrence after radical prostatectomy and external-beam radiotherapy [37, 38]. In patients after primary radiation therapy, a combination of both DCE-MRI and DWI is regarded as most efficient [37].

For the detection of bone metastases, ^{11}C-choline PET/CT and PET/MR performed equally well in patients with a PSA value ≤2 ng/ml. However, PET/CT was more efficient in the subgroup of patients with PSA values >2 ng/ml. This was a rather unexpected finding and not predicted, as usually MRI is regarded as the modality of choice for assessment of bone lesions. A potential explanation is that most bone metastases are osteoblastic, offering a clear morphological correlate on CT. In contrast, whole-body MR sequences as also used in PET/MR are often (a) in coronal plane, due to faster acquisition, and (b) are usually acquired in thicker sections with a higher intersection gap. Both facts could lead to less confident reporting, as imaging specialists are more used to reading axial slices and small lesions are easier to be missed in thicker slices.

Finally, the observation of this difference only in PSA values >2 ng/ml is merely related to the lower incidence of bone metastases in low PSA values.

For the detection of lymph node metastases, ^{11}C-choline PET has considerable incremental value to morphological imaging, as CT and MRI still mainly rely on size and shape with its well-known limitations and even mpMR is not of incremental value [36, 39]. Scattoni et al. evaluating ^{11}C-choline PET/CT in recurrent PC reported a lesion-based sensitivity and specificity of 64 and 90%, respectively [40]. Correspondingly, in our study, no difference was present in the detection of lymph node metastases between ^{11}C-choline PET/CT and PET/MR for patients with a PSA value ≤2 ng/ml. However, interestingly, in the subgroup of patients with PSA values >2 ng/ml, ^{11}C-choline PET/CT was even more efficient in detecting lymph node metastases. Potential reasons could again be related to the imaging technique for whole-body MRI. Diagnostic multi-slice CT acquisition with multi-planar reconstructions has a clear advantage for displaying small structures. Thus, in our experience it was easier to attribute areas of slightly increased ^{11}C-choline uptake to small lymph nodes using CT compared to MRI. By investing more time in image acquisition in the pelvis in MRI, a higher resolution could be achieved, which has now been implemented in our routine

protocol. However, further improvements in MR technology (e.g., continuous table movement) might also allow application of new more time-efficient sequences in PET/MR, facilitating the detection and anatomical allocation of small lesions [41].

From an interpretative point of view, ^{11}C-choline PET/MR can be regarded as a robust modality for restaging PC with high inter-observer and intra-modality agreement for the most items analyzed and in the range for other imaging modalities [42–46]. As expected, mean imaging time for PET/CT was significantly lower compared to PET/MR, which is clearly related to our comprehensive MR protocol. In fact, the significantly lower imaging time of PET/CT combined with the lack of whole-body surface coils makes PET/CT clearly more convenient for the patient. In addition, PET/MR reading is more time consuming. Contrarily, the simulated mean reduction in effective dose for PET/MR of 13.84 mSv is considerable, equaling 3–5 times the natural background radiation. However, radiation dose calculations are approximations and not precise measures of an individual's radiation dose and reduction of effective dose is less relevant in an elderly patients with cancer.

Our study has several limitations. First, histopathology was available in only a minority of patients which, however, is a common issue in this setting as often neither easily feasible nor justified ethically. Second, the sequence of performing PET/CT first followed by PET/MR was determined by our IRB approval, but could introduce bias. Third, no separate analysis of the diagnostic capability of both PET components and/or CT vs. MRI components was performed, as our intention was to compare the value of both hybrid examinations. Nevertheless, prior studies showed relatively identical performance of both PET components for ^{11}C-choline [32, 33]. Souvatzoglou et al. reported no significant difference between ^{11}C-choline PET/MR and PET/CT for lesion detection. Only single lesions could be identified by PET/CT only potentially being missed due to the lower counts in subsequent PET/MR. Similarly, we cannot exclude that the performance of PET/MR was potentially deteriorated by the later imaging point for PET/MR. Finally, the recent, successful, and widespread clinical adoption of PSMA ligands has overcome some limitations and resulted in clearly increased detection rates. However, the first data still indicate that mpMR within the use of PET/MR has its specific value in the detection of local recurrence, which can also be missed by ^{68}Ga-PSMA HBED-CC PET imaging alone [47].

Conclusions

[11]C-choline PET/MR is robust for restaging or recurrent PC and provides higher diagnostic value for detecting local recurrence compared to PET/CT. Drawbacks are a substantially longer imaging time as well as a slight inferiority in detecting

bone and lymph node metastases in patients with PSA values >2 ng/ml. Thus, we suggest using PET/MR primarily for the patient group with low-level PSA recurrence, while PET/CT is preferable in patients with higher-level PSA recurrence. The potential advantage of a considerable less radiation dose is less relevant in this particular patient collective.

References

1. Ferlay J, Steliarova-Foucher E, Lortet-Tieulent J, et al. Cancer incidence and mortality patterns in Europe: estimates for 40 countries in 2012. Eur J Cancer. 2013;49:1374–403.
2. Garnick MB, Fair WR. Combating prostate cancer. Sci Am. 1998;279:74–83.
3. Freedland SJ, Presti JC Jr, Amling CL, et al. Time trends in biochemical recurrence after radical prostatectomy: results of the SEARCH database. Urology. 2003;61:736–41.
4. Han M, Partin AW, Zahurak M, Piantadosi S, Epstein JI, Walsh PC. Biochemical (prostate specific antigen) recurrence probability following radical prostatectomy for clinically localized prostate cancer. J Urol. 2003;169:517–23.
5. Chism DB, Hanlon AL, Horwitz EM, Feigenberg SJ, Pollack A. A comparison of the single and double factor high-risk models for risk assignment of prostate cancer treated with 3D conformal radiotherapy. Int J Radiat Oncol Biol Phys. 2004;59:380–5.
6. Krause BJ, Souvatzoglou M, Tuncel M, et al. The detection rate of [11C]choline-PET/CT depends on the serum PSA value in patients with biochemical recurrence of prostate cancer. Eur J Nucl Med Mol Imaging. 2008;35:18–23.
7. de Jong IJ, Pruim J, Elsinga PH, Vaalburg W, Mensink HJ. Preoperative staging of pelvic lymph nodes in prostate cancer by 11C-choline PET. J Nucl Med. 2003;44:331–5.
8. Krause BJ, Souvatzoglou M, Treiber U. Imaging of prostate cancer with PET/CT and radioactively labeled choline derivates. Urol Oncol. 2013;31:427–35.
9. Beer AJ, Eiber M, Souvatzoglou M, Schwaiger M, Krause BJ. Radionuclide and hybrid imaging of recurrent prostate cancer. Lancet Oncol. 2011;12:181–91.
10. Castellucci P, Fuccio C, Nanni C, et al. Influence of trigger PSA and PSA kinetics on 11C-choline PET/CT detection rate in patients with biochemical relapse after radical prostatectomy. J Nucl Med. 2009;50:1394–400.
11. Giovacchini G, Picchio M, Coradeschi E, et al. [(11)C]choline uptake with PET/CT for the initial diagnosis of prostate cancer: relation to PSA levels, tumour stage and anti-androgenic therapy. Eur J Nucl Med Mol Imaging. 2008;35:1065–73.
12. Evangelista L, Briganti A, Fanti S, et al. New clinical indications for (18)F/(11)C-choline, new tracers for positron emission tomography and a promising hybrid device for prostate cancer staging: a systematic review of the literature. Eur Urol. 2016;70:161–75.
13. Heidenreich A, Bastian PJ, Bellmunt J, et al. EAU guidelines on prostate cancer. Part 1: screening, diagnosis, and local treatment with curative intent-update 2013. Eur Urol. 2013;65:124–37.
14. Seemann MD. Whole-body PET/MRI: the future in oncological imaging. Technol Cancer Res Treat. 2005;4:577–82.
15. Antoch G, Bockisch A. Combined PET/MRI: a new dimension in whole-body oncology imaging? Eur J Nucl Med Mol Imaging. 2009;36(Suppl 1):S113–20.
16. Boonsirikamchai P, Choi S, Frank SJ, et al. MR imaging of prostate cancer in radiation oncology: what radiologists need to know. Radiographics. 2013;33:741–61.
17. Vargas HA, Wassberg C, Akin O, Hricak H. MR imaging of treated prostate cancer. Radiology. 2012;262:26–42.
18. Kim CK, Park BK, Lee HM. Prediction of locally recurrent prostate cancer after radiation therapy: incremental value of 3T diffusion-weighted MRI. J Magn Reson Imaging. 2009;29:391–7.
19. Haider MA, Chung P, Sweet J, et al. Dynamic contrast-enhanced magnetic resonance imaging for localization of recurrent prostate cancer after external beam radiotherapy. Int J Radiat Oncol Biol Phys. 2008;70:425–30.
20. Eiber M, Takei T, Souvatzoglou M, et al. Performance of whole-body integrated 18F-FDG PET/MR in comparison to PET/CT for evaluation of malignant bone lesions. J Nucl Med. 2014;55:191–7.
21. Rauscher I, Eiber M, Furst S, et al. PET/MR imaging in the detection and characterization of pulmonary lesions: technical and diagnostic evaluation in comparison to PET/CT. J Nucl Med. 2014;55:724–9.
22. Bailey DL, Pichler BJ, Guckel B, et al. Combined PET/MRI: multimodality multi-parametric imaging is here: summary report of the 4th international workshop on PET/MR imaging; February 23-27, 2015, Tubingen, Germany. Mol Imaging Biol. 2015;17:595–608.
23. Delso G, Furst S, Jakoby B, et al. Performance measurements of the Siemens mMR integrated whole-body PET/MR scanner. J Nucl Med. 2011;52:1914–22.
24. Drzezga A, Souvatzoglou M, Eiber M, et al. First clinical experience with integrated whole-body PET/MR: comparison to PET/CT in patients with oncologic diagnoses. J Nucl Med. 2012;53:845–55.
25. Tolvanen T, Yli-Kerttula T, Ujula T, et al. Biodistribution and radiation dosimetry of [(11)C]choline: a comparison between rat and human data. Eur J Nucl Med Mol Imaging. 2010;37:874–83.
26. Huda W, Ogden KM, Khorasani MR. Converting dose-length product to effective dose at CT. Radiology. 2008;248:995–1003.
27. European Guidelines on Quality Criteria for Computed Tomography. Report EUR 16262. Brussels, Belgium: European Commission; 1999.
28. Brix G, Lechel U, Glatting G, et al. Radiation exposure of patients undergoing whole-body dual-modality 18F-FDG PET/CT examinations. J Nucl Med. 2005;46:608–13.
29. Huda W, Magill D, He W. CT effective dose per dose length product using ICRP 103 weighting factors. Med Phys. 2011;38:1261–5.
30. Svanholm H, Starklint H, Gundersen HJ, Fabricius J, Barlebo H, Olsen S. Reproducibility of histomorphologic diagnoses with special reference to the kappa statistic. APMIS. 1989;97:689–98.
31. Tuncel M, Souvatzoglou M, Herrmann K, et al. [(11)C]choline positron emission tomography/computed tomography for staging and restaging of patients with advanced prostate cancer. Nucl Med Biol. 2008;35:689–95.
32. Souvatzoglou M, Eiber M, Takei T, et al. Comparison of integrated whole-body [11C]choline PET/MR with PET/CT in patients with prostate cancer. Eur J Nucl Med Mol Imaging. 2013;40:1486–99.

33. Wetter A, Lipponer C, Nensa F, et al. Simultaneous 18F choline positron emission tomography/magnetic resonance imaging of the prostate: initial results. Investig Radiol. 2013;48:256–62.

34. Wetter A, Lipponer C, Nensa F, et al. Quantitative evaluation of bone metastases from prostate cancer with simultaneous [18F] choline PET/MRI: combined SUV and ADC analysis. Ann Nucl Med. 2014;28:405–10.

35. Wetter A, Nensa F, Schenck M, et al. Combined PET imaging and diffusion-weighted imaging of intermediate and high-risk primary prostate carcinomas with simultaneous [18F] choline PET/MRI. PLoS One. 2014;9:e101571.

36. Kitajima K, Murphy RC, Nathan MA, et al. Detection of recurrent prostate cancer after radical prostatectomy: comparison of 11C-choline PET/CT with pelvic multiparametric MR imaging with endorectal coil. J Nucl Med. 2014;55:223–32.

37. Roy C, Foudi F, Charton J, et al. Comparative sensitivities of functional MRI sequences in detection of local recurrence of prostate carcinoma after radical prostatectomy or external-beam radiotherapy. AJR Am J Roentgenol. 2013;200:W361–8.

38. Panebianco V, Sciarra A, Lisi D, et al. Prostate cancer: 1HMRS-DCEMR at 3T versus [(18)F]choline PET/CT in the detection of local prostate cancer recurrence in men with biochemical progression after radical retropubic prostatectomy (RRP). Eur J Radiol. 2012;81:700–8.

39. Hovels AM, Heesakkers RA, Adang EM, et al. The diagnostic accuracy of CT and MRI in the staging of pelvic lymph nodes in patients with prostate cancer: a meta-analysis. Clin Radiol. 2008;63:387–95.

40. Scattoni V, Picchio M, Suardi N, et al. Detection of lymph-node metastases with integrated [11C]choline PET/CT in patients with PSA failure after radical retropubic prostatectomy: results confirmed by open pelvic-retroperitoneal lymphadenectomy. Eur Urol. 2007;52:423–9.

41. Brauck K, Zenge MO, Vogt FM, et al. Feasibility of whole-body MR with T2- and T1-weighted real-time steady-state free precession sequences during continuous table movement to depict metastases. Radiology. 2008;246:910–6.

42. Fendler WP, Barrio M, Spick C, et al. 68Ga-DOTATATE PET/CT interobserver agreement for neuroendocrine tumor assessments: results of a prospective study on 50 patients. J Nucl Med. 2017;58(2):307–11.

43. Ruf J, Schiefer J, Furth C, et al. 68Ga-DOTATOC PET/CT of neuroendocrine tumors: spotlight on the CT phases of a triple-phase protocol. J Nucl Med. 2011;52:697–704.

44. Muller BG, Shih JH, Sankineni S, et al. Prostate cancer: Interobserver agreement and accuracy with the revised prostate imaging reporting and data system at multiparametric MR imaging. Radiology. 2015;277:741–50.

45. Senft A, de Bree R, Golding RP, et al. Interobserver variability in chest CT and whole body FDG-PET screening for distant metastases in head and neck cancer patients. Mol Imaging Biol. 2010;13:385–90.

46. Thureau S, Chaumet-Riffaud P, Modzelewski R, et al. Interobserver agreement of qualitative analysis and tumor delineation of 18F-fluoromisonidazole and 3′-deoxy-3′-18F-fluorothymidine PET images in lung cancer. J Nucl Med. 2013;54:1543–50.

47. Freitag MT, Radtke JP, Hadaschik BA, et al. Comparison of hybrid (68)Ga-PSMA PET/MRI and (68)Ga-PSMA PET/CT in the evaluation of lymph node and bone metastases of prostate cancer. Eur J Nucl Med Mol Imaging. 2016;43:70–83.